Ultraviolet band edge photorefractivity in $LiNbO_3$:Sn crystals

Feifei Xin,[1,2,3] Guoquan Zhang,[1,3,*] Xinyu Ge,[1] Shiguo Liu,[1] Li Xuan,[2] Yongfa Kong,[1,3] and Jingjun Xu[1,2,3]

[1]*The MOE Key Laboratory of Weak Light Nonlinear Photonics, Nankai University, Tianjin 300457, China*

[2]*State Key Laboratory of Applied Optics, Changchun Institute of Optics, Fine Mechanics and Physics, Chinese Academy of Sciences, Changchun 130033, China*

[3]*Photonics Center, School of Physics, Nankai University, Tianjin 300071, China*

**Corresponding author: zhanggq@nankai.edu.cn*

Received June 7, 2011; revised July 15, 2011; accepted July 16, 2011; posted July 18, 2011 (Doc. ID 148888); published August 11, 2011

The ultraviolet (UV) band edge photorefractivity of Sn-doped $LiNbO_3$ (LN:Sn) at 325 nm has been investigated. A sharp decrease of beam distortion, which is accompanied by a significant increase in the photoconductivity, is observed in LN:Sn crystals with Sn-doping concentrations at or above 2.0 mol%. The diffraction efficiency, the holographic recording sensitivity and response rate, and the two-wave coupling gain coefficient are greatly enhanced when the Sn-doping concentration reaches 2.0 mol% or more. Unlike $LiNbO_3$ doped with Hf in which the UV gratings can be erased easily by a red beam, the UV gratings in LN:Sn can withstand long-term red beam illumination. Electrons are determined to be the dominant light-induced charge carriers responsible for the UV band edge photorefraction. The observed enhancement on the UV band edge photorefractivity is found to be associated with the showup of an absorption band around 325 nm in LN:Sn crystals with Sn-doping concentrations at or above 2.0 mol%.

OCIS codes: 160.5320, 190.5330, 090.7330, 160.3730.

Lithium niobate ($LiNbO_3$, LN) crystal is one of the most widely used photorefractive materials [1]. The optical properties of LN can be modified largely with different dopants. Dopants such as Fe, Mn, and Cu act as photorefractive centers in the visible, whereas the effect of Mg, Zn, and In on the photorefraction depends on the operating light wavelength. It was found that the so-called optical damage resistant ions in the visible such as Mg, Zn, and In induce a great enhancement on photorefractivity in the UV [2–5]. Recently, tetravalent dopants such as Hf^{4+}, Zr^{4+} and Sn^{4+} were found to be optical damage resistant ions in the visible with very low threshold doping concentrations and distribution coefficient close to 1.0 [6–9]. However, when it comes to the UV region, things become much more complicated. For example, Hf-doped LN with a doping concentration higher than 2.5 mol% possesses an enhanced UV photorefraction, while Zr-doped LN remains optical damage resistant at 351 nm [10,11]. However, the effect of Sn^{4+} ions on the UV photorefraction, especially that near to the band edge, remains unknown. In this Letter, we report on the UV band edge photorefractivity of LN:Sn.

Samples used in the study were congruent LN crystals doped with 0.0, 1.0, 2.0, 2.5, 3.5, 4.0, 4.5, and 5.0 mol% SnO_2, and therefore labeled as CLN, CSn1, CSn2, CSn2.5, CSn3.5, CSn4, CSn4.5, and CSn5, respectively. The crystals were grown along the crystallographic *c*-axis by the Czochralski method. *Y*-oriented plates with a thickness of 3 mm were cut and polished to optical grade. Beam distortion and two-wave coupling techniques were employed to characterize the UV band edge photorefractivity at 325 nm.

In the beam distortion experiment, an *e*-polarized beam operating at 325 nm from a He-Cd laser was focused into the sample. The intensity at the focal point was 900 kW/cm^2. Figure 1 shows the transmitted beam spot after CLN and LN:Sn samples for a 5 min irradiation. Similar to the results in LN-doped with Hf and Zr [10,11], the beam distortion in our samples decreases with the increase of the Sn-doping concentration. This indicates that the photovoltaic field weakens owing to the increase of the photoconductivity induced by Sn-doping. In particular, a sharp decrease in beam distortion occurs when the Sn-doping concentration reaches 2.0 mol%.

We used the two-wave coupling configuration to study the UV band edge photorefraction of our samples. Two *e*-polarized coherent beams at 325 nm with equal intensities 490 mW/cm^2 were intersected in the sample with a crossing angle of 32° in air. The grating wave vector was aligned along the *c*-axis of the sample. A third beam at 325 nm, expanded and incident at an off-Bragg angle when necessary, was served as a uniform erasing beam. The buildup and decay dynamics of the gratings were monitored by a weak red probe beam at 633 nm incident at the Bragg-matched angle. The probe beam intensity was kept as low as 2 mW/cm^2 in order to avoid any detectable effect on the grating buildup and decay dynamics. During the measurement, we launched the two writing beams and the weak probe beam onto the crystal synchronously. After the diffracted beam intensity of the probe beam reached a saturated value, we turned off the two writing beams and launched the uniform UV erasing beam of 32.6 mW/cm^2 onto the crystal at the same time to study the erasing dynamics of the gratings.

Figure 2 shows the UV band edge photorefraction of investigated samples, where the definitions of the characteristic parameters can be found in [4,12] and

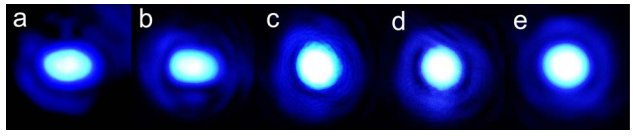

Fig. 1. (Color online) Transmitted beam spots of a 900 kW/cm^2 UV beam after a 5 min irradiation. (a–e) correspond to the cases for LN doped with 0.0, 1.0, 2.0, 3.5, and 5.0 mol% SnO_2.

textbooks such as [1,13]. One can see that the photorefractive properties of LN:Sn with Sn-doping concentrations at or above 2.0 mol% are dramatically improved. An abrupt increase in diffraction efficiency from ~6.0% to ~40.0% [Fig. 2(a)], a sharp drop of the buildup response time from ~6.00 s to ~0.25 s [Fig. 2(b)], and a significant increase in the holographic recording sensitivity [for ~30 times, see Fig. 2(c)] appear between the samples CLN and CSn1 and those with Sn-doping concentrations at or above 2.0 mol%. As the beam distortion experiment suggested, the photoconductivity σ_{ph} of LN would be greatly increased by Sn-doping at or above 2.0 mol%. To verify this, we measured the specific photoconductivity σ_{ph}/I_e, where σ_{ph} was estimated through the relationship $\sigma_{ph} = \epsilon_0\epsilon/\tau_e$ with ϵ_0 and ϵ being the electric permeability of vacuum and relative static dielectric constant, and τ_e being the erasing time constant of gratings erased by a UV erasing beam of intensity I_e [1,4], respectively. The results, shown in Fig. 2(d), confirm the above hypothesis. It should be noticed that, although the photorefraction in the UV is improved significantly whereas that in the visible is suppressed dramatically with the increase of Sn-doping concentration [9], both of them show a concentration threshold effect.

In the measurement of the two-wave coupling gain coefficient, we set the intensity ratio between the strong pump beam and the weak signal beam to be 100∶1. As shown in Fig. 3, the two-wave coupling gain has the similar behavior as other parameters, showing a sudden increase in sample CSn2 and then keeping nearly the same as the Sn-doping concentration continues to increase. We observed that the light energy was transferred unidirectionally towards $-c$-axis in all samples in the two-wave coupling process, indicating that diffusion is the dominant charge transport mechanism and electrons are the dominant light-induced charge carriers during the UV band edge photorefractive processes in LN:Sn [13].

Interestingly, we found that the UV band edge photorefractive gratings recorded in LN:Sn can withstand long-term red irradiation. To study the decay dynamics of the

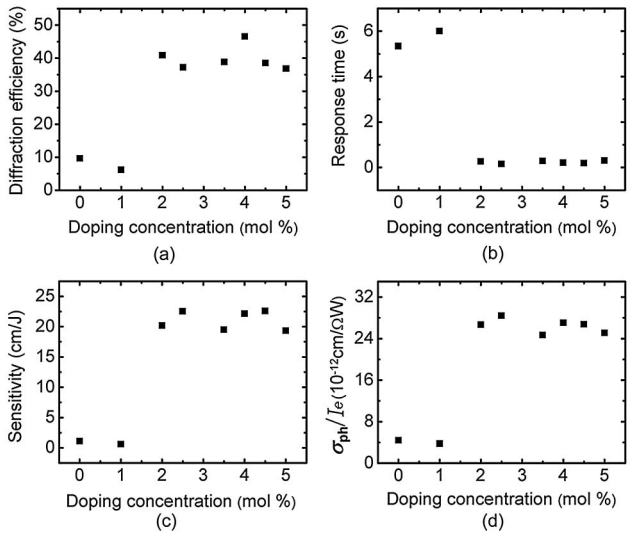

Fig. 2. Dependence of UV band edge photorefractive (a) diffraction efficiency, (b) response time, (c) sensitivity, and (d) specific photoconductivity on the doping concentration of Sn.

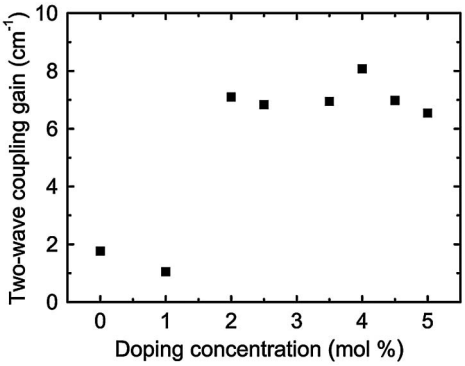

Fig. 3. Dependence of UV band edge photorefractive two-wave coupling gain on the Sn-doping concentration.

UV band edge gratings in LN:Sn, we increased the intensity of the red monitoring beam up to 82.7 mW/cm^2 after the UV band edge holographic grating recording. Figure 4 shows a typical decay dynamic of the UV band edge photorefractive gratings in CSn4, in which the diffraction efficiency is normalized. One sees that the diffraction efficiency decreases quickly by an amount of ~16% and then levels off even for a long-term red beam irradiation. On the other hand, the UV band edge gratings were confirmed to be stable in the dark. The grating decay dynamics for other samples are similar. This result is very different from that reported in highly Hf-doped LN crystals, in which the UV gratings recorded at 351 nm are completely erased by red irradiation [10]. It was suggested that in LN:Hf crystals unintentional Fe ions serve as the shallow level which traps all the UV excited electrons to build up the UV gratings. The nonvolatility of the remaining UV band edge photorefractive grating at 633 nm in our cases indicates that there are other deep level traps playing a key role in the UV band edge photorefractive processes in LN:Sn crystals. One notes that the remaining UV band edge gratings in LN:Sn can be easily erased by the UV erasing beam at 325 nm, as shown in Fig. 4.

One notes that the operating wavelength in our experiments is very close to the UV absorption edge of LN:Sn, therefore, it is necessary to measure the fine spectral structure of the absorption spectra near to the absorption edge. It was found that the room-temperature absorption spectra for all samples were similar. Fortunately, we

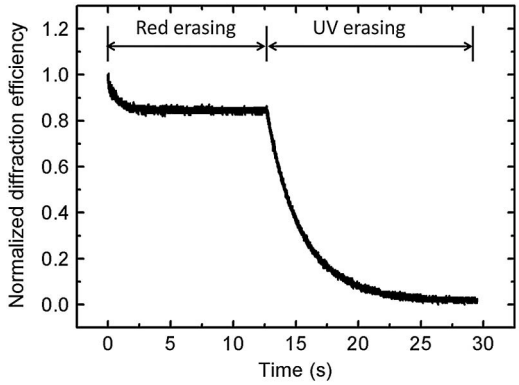

Fig. 4. The decay dynamics of the UV band edge photorefractive gratings in CSn4 under the erasure of red beam of 82.7 mW/cm^2 at 633 nm and UV beam of 32.6 mW/cm^2 at 325 nm in sequence.

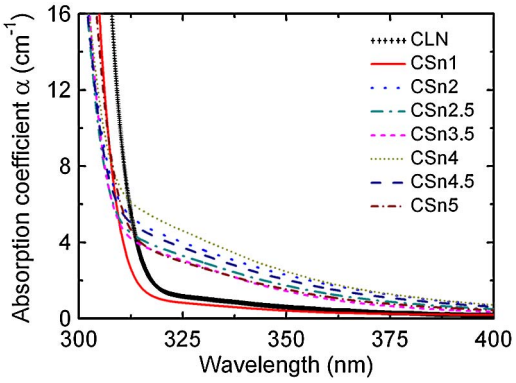

Fig. 5. (Color online) UV absorption spectra of congruent undoped LN and LN:Sn crystals at 3.8 K.

found that the UV absorption edge of LN:Sn is quite sensitive to the crystal temperature and a significant UV shift in the absorption edge occurs in LN:Sn when one decreases the crystal temperature. Therefore, it is possible to show the fine spectral structure near to the absorption edge of LN:Sn by measuring the absorption spectra at cryogenic temperature. Figure 5 shows the absorption spectra of our samples at a cryogenic temperature of 3.8 K. Note that an absorption shoulder covering the wavelength of 325 nm shows up in all LN:Sn crystals with Sn-doping concentration at or above 2.0 mol%. Thus, combining with the observed UV band edge photorefractive properties, it is reasonable to deduce that it is the defect structure corresponding to this absorption shoulder that is responsible for the UV band edge photorefractive process in LN:Sn. However, more detailed studies are necessary to finally identify the responsible defect, which are currently under the way in our laboratory.

In summary, the UV band edge photorefractivity of a series of Sn-doped LN was investigated by beam distortion and two-wave coupling techniques. The UV band edge photorefractive properties of LN are greatly improved by doping Sn up to 2.0 mol% or more. Electrons are determined to be the dominant charge carriers responsible for the UV band edge photorefraction. Moreover, the UV band edge photorefractive gratings remain nonvolatile under long-term red irradiation, indicating that deep level centers other than unintentional Fe ions dominate the buildup of the UV holographic gratings in LN:Sn. The UV absorption spectra at cryogenic temperatures reveal the showup of an absorption band covering the wavelength of 325 nm in highly Sn-doped LN, which may attribute to the deep level centers responsible for the UV band edge photorefraction. Our experimental results also suggest that LN:Sn is a promising UV photorefractive material with the advantages of low-doping concentration, fast response speed, strong resistance to beam distortion, and acceptable diffraction efficiency.

This work is supported by the Ministry of Education (MOE) Cultivation Fund of the Key Scientific and Technical Innovation Project (708022), the National Natural Science Foundation of China (NSFC) (90922030, 10 804 054, 10 904 077), the 973 Program (2007CB307002), the Chinese National Key Basic Research Special Fund (CNKBRSF) (2011CB922003), the 111 Project (B07013), and the Fundamental Research Funds for the Central Universities.

References

1. T. Volk and M. Wöhlecke, *Lithium Niobate: Defects, Photorefraction and Ferroelectric Switching* (Springer-Verlag, Berlin, 2008).
2. R. Jungen, G. Angelow, F. Laeri, and C. Grabmaier, Appl. Phys. A **55**, 101 (1992).
3. J. Xu, G. Zhang, F. Li, X. Zhang, Q. Sun, S. Liu, F. Song, Y. Kong, X. Chen, H. Qiao, J. Yao, and L. Zhao, Opt. Lett. **25**, 129 (2000).
4. H. Qiao, J. Xu, G. Zhang, X. Zhang, Q. Sun, and G. Zhang, Phys. Rev. B **70**, 094101 (2004).
5. F. Xin, G. Zhang, F. Bo, H. Sun, Y. Kong, J. Xu, T. Volk, and N. Rubinina, J. Appl. Phys. **107**, 033113 (2010).
6. E. P. Kokanyan, L. Razzari, I. Cristiani, V. Degiorgio, and J. B. Gruber, Appl. Phys. Lett. **84**, 1880 (2004).
7. L. Razzari, P. Minzioni, I. Cristiani, V. Degiorgio, and E. Kokanyan, Appl. Phys. Lett. **86**, 131914 (2005).
8. Y. Kong, S. Liu, Y. Zhao, H. Liu, S. Chen, and J. Xu, Appl. Phys. Lett. **91**, 081908 (2007).
9. L. Wang, S. Liu, Y. Kong, S. Chen, Z. Huang, L. Wu, R. Rupp, and J. Xu, Opt. Lett. **35**, 883 (2010).
10. W. Yan, L. Shi, H. Chen, X. Zhang, and Y. Kong, Opt. Lett. **35**, 601 (2010).
11. F. Liu, Y. Kong, W. Li, H. Liu, S. Liu, S. Chen, X. Zhang, R. Rupp, and J. Xu, Opt. Lett. **35**, 10 (2009).
12. G. C. Valley and M. B. Klein, Opt. Eng. (Bellingham, Wash.) **22**, 704 (1983).
13. L. Solymar, D. J. Webb, and A. Grunnet-Jepsen, *The Physics and Applications of Photorefractive Materials* (Oxford University Press, New York, 1996).